Gold Nanoparticle-Assisted Laser Surface Modification of Borosilicate Glass Substrates

Shuichi Hashimoto,*,† Takayuki Uwada,‡,§ Masahide Hagiri,|| Hiroaki Takai,† and Tomoyuki Ueki†

Department of Ecosystem Engineering, The University of Tokushima, Tokushima 770-8506, Japan, Department of Applied Chemistry and Institute of Molecular Science, National Chiao Tung University, Hsinchu 30010, Taiwan, Graduate School of Materials Science, Nara Institute of Science and Technology (NAIST), Ikoma 630-0192, Japan, and Department of Chemistry and Biochemistry, Fukushima National College of Technology, Iwaki 970-8034, Japan

Received: June 5, 2009; Revised Manuscript Received: August 24, 2009

This paper describes the photomodification of borosilicate glass substrates assembled with 40 nm diameter gold nanoparticles (Au NPs) with surface coverages ranging from 17 to 23% on excitation of the localized surface plasmon band of the NPs with a 532 nm nanosecond pulsed-laser beam. The laser irradiation allowed the splitting and fusion of NPs on the substrate surface and, at the same time, the formation of craters of less than 10 nm diameter at various places following one laser shot with a relatively high intensity of 460 or 370 $mJ \cdot cm^{-2} \cdot pulse^{-1}$ but well below the breakdown threshold of 25−40 $J \cdot cm^{-2} \cdot pulse^{-1}$. The formation of the craters was more and more distinctly observed by continuous irradiations. The number density, average diameter, and the surface coverage of the craters were not linearly dependent on the laser shot number but exhibited the saturation behavior due to the consumption of Au NPs. The threshold laser energy for the crater formation was dependent on the accumulated number of laser shots: a greater number of laser shots were necessary to form craters as the laser fluence decreases. Most interestingly, the laser-irradiated areas of the substrate exhibited a greater susceptibility to the wet chemical etching with aqueous hydrogen fluoride. The mechanism of the laser modification and a possible application to nanofabrication on glass surfaces by utilizing Au NPs were discussed on the basis of the scanning electron microscopy (SEM) observation as well as the extinction and light scattering spectroscopic measurements.

Introduction

Laser material processing technique has attracted a great deal of attention as a tool for top-down micro- and nanofabrication of various metallic, inorganic, and polymer solids as well as photopolymers including photoresists.[1] In particular, the processing of transparent materials such as glasses has been realized by exposure to both ultraviolet nanosecond lasers and near-infrared femtosecond lasers. The former was applied mainly to structure the surface of the UV absorbing materials, while the latter was exploited to modify inside the materials assisted by a multiphoton absorption process.[2,3] The laser technique is powerful and versatile when used to a microscale 3D structuring; however, the method suffers from a serious drawback such as very low throughput or high photon cost because only a small portion of photons injected is actually used for the processing and most of the photons are wasted. To overcome this problem, the electric field enhancement exploiting the surface plasmon coupling of noble metal nanoparticles (NPs)[4] is promising especially for nanoscale fabrications. An additional benefit to take advantage of the plasmonic enhancement is the availability of high throughput visible lasers that have not been applied to the processing of transparent materials because of low absorption efficiencies. Thus an investigation aiming at utilizing NPs to laser material structuring is of high importance not only for expanding the capability of nanomaterial-based technology to a new field but also for developing energy-saving ways of laser fabrication.

Noble metal NPs have attracted widespread interest because of unusual optical properties[4] that find applications such as plasmonic devices,[5−7] biosensors,[8,9] nonlinear optics,[10,11] and ultratrace analyses based upon surface-enhanced Raman scattering (SERS).[12,13] In particular, the filed enhancement in the near-field regime on excitation of the localized surface plasmon band of Ag and Au allowed the remarkable enhancement of Raman scattering[12,13] and fluorescence[14,15] signals for molecules residing in the close vicinities of the particles. Contrastingly, less attention has been paid to the laser micro- and nanofabrication exploiting NPs. Only a few studies have focused on NP-assisted laser nanofabrication. For instance, Obara and co-workers observed the formation of nanoholes on the surface of a silicon substrate placed with 200 nm diameter Au spheres by irradiating a single femtosecond laser pulse (800 nm) with an intensity of less than the ablation threshold of silicon.[16−18] Leiderer and co-workers also observed the ablation pattern for regular arrays of gold triangles with a side length of 450 and 25 nm thickness when these structures were illuminated with a laser pulse of 150 fs (800 nm, 10 $mJ \cdot pulse^{-1}$).[19] Holes as small as 5 nm were formed at two corners of each triangle on a silicon substrate. Helzel and co-workers observed nanoholes of roughly the diameter of spheres or slightly smaller on silicon surface placed with 250 and 40 nm Au nanospheres and exposed to a single pulse of 532 nm nanosecond laser.[20] These groups ascribed their findings to the plasmonic enhancement of the incident electric field at the boundary of the NP and the substrate. In contrast to these studies, Tsuboi and co-workers

* Corresponding author. E-mail: hashi@eco.tokushima-u.ac.jp.
† The University of Tokushima.
‡ National Chiao Tung University.
§ Nara Institute of Science and Technology (NAIST).
|| Fukushima National College of Technology.

10.1021/jp905291h CCC: $40.75
Published on Web 11/10/2009

gave a view distinct from the previous one to the observation of nanohole (d < 100 nm) formation on a Au NP−polymer hybrid film deposited on glass substrates and irradiated by a single 532 nm laser shot.[21] They ascribed the origin of the nanoholes, not to the plasmonic enhancement, but to the laser heating exceeding the boiling point of Au. Despite the fact that nanohole fabrication on silicon surface has been reported upon the laser excitation of Au NPs, the fabrication on a glass substrate has rarely been investigated. This is because the laser processing of a glass substrate by the application of an NP-based approach is a more challenging task than the fabrication on a silicon substrate where a larger plasmonic enhancement is predicted because of its greater dielectric functions.

Our research strategy consists of three stages: first, the laser nanofabrication on the glass surface assembled with Au NPs in analogy with the previous works on silicon substrates. Second, the laser fabrication can be attempted inside the glass substrates containing Au NPs. Previously, a SiO_2-thin film containing Au NPs of 2−20 nm diameter irradiated with a 351 nm laser (0.5 ns pulse width, 2−5 J·cm^{-2}·pulse^{-1}) allowed the formation of nanoscale craters approximately 10 times larger than the size of the NPs.[22] The investigation was intended to assess the reduction in the damage threshold of optical materials due to impurities, but also demonstrated that the method is better suited for a nanoscale fabrication inside the glass than the light-absorbing ion doping method.[23] Third, the fabrication of groove structures can be performed based upon a laser-induced backside wet etching (LIBWE) technique. The LIBWE technique developed by Niino and co-workers promotes the energy deposition of UV lasers to a thin layer at the glass-dye solution interface through the ablation of the solution, leading to the etching from the glass surface to the inside.[24] The important difference from the original method is the use of Au NP solution that can absorb a visible laser light, allowing the use of a 532 nm beam from nanosecond YAG lasers. Here we report an initial attempt of laser-modification of glass surfaces followed by the wet chemical etching of the modified area. We employed glass substrates deposited with Au NPs ranging from 15 to 70 nm and inspected the morphological changes of both the NPs and the glass surface on irradiation with a 532 nm nanosecond laser. We found that laser-modified areas are susceptible to etching by hydrofluoric acid (HF) and thus demonstrated the possibility of laser fabrication exploiting Au NPs. Furthermore, the mechanistic aspect of the Au NP-assisted visible laser photomodification will be described.

Experimental Section

The procedure for gold NP preparation was described elsewhere.[25] Gold NPs were assembled on 3-aminopropyltriethoxysilane (APTES)-functionalized coverslip (Matsunami, borosilicate glass) surfaces.[26] Briefly, glass substrates (18 × 18 × 0.5) cleaned by submerging in a 1:1 mixture of ammonia−water (28%) and aqueous hydrogen peroxide (30%) and dried were treated with a 2% methanol solution of APTES for 1 h at 60 °C. After three runs of separate washing in methanol and distilled water, with sonication each for 1 min, the substrates were allowed to stand in an aqueous Au NP solution for 3−24 h at 4−5 °C. The substrates assembled with Au NP films were rinsed with distilled water.

Laser irradiation was carried out normal to a glass substrate by the unfocused beam of a frequency-doubled output (532 nm) of a nanosecond Nd:YAG laser (Continuum: Surelite I-10, pulse width: 6 ns; repetition rate; 10 Hz). The resultant glass substrates were examined by extinction spectroscopy (Hitachi, U-2010 spectrophotometer), light scattering spectroscopy (Hamamatsu, PMA-12 CCD multichannel spectrophotometer), and field emission scanning electron microscopy (FE-SEM, Hitachi S4700). For the observation of FE-SEM of glass substrates, Pt−Pd alloy was sputter deposited. The sputtered particles were distinguished from Au particles because of their size of less than 5 nm diameter.

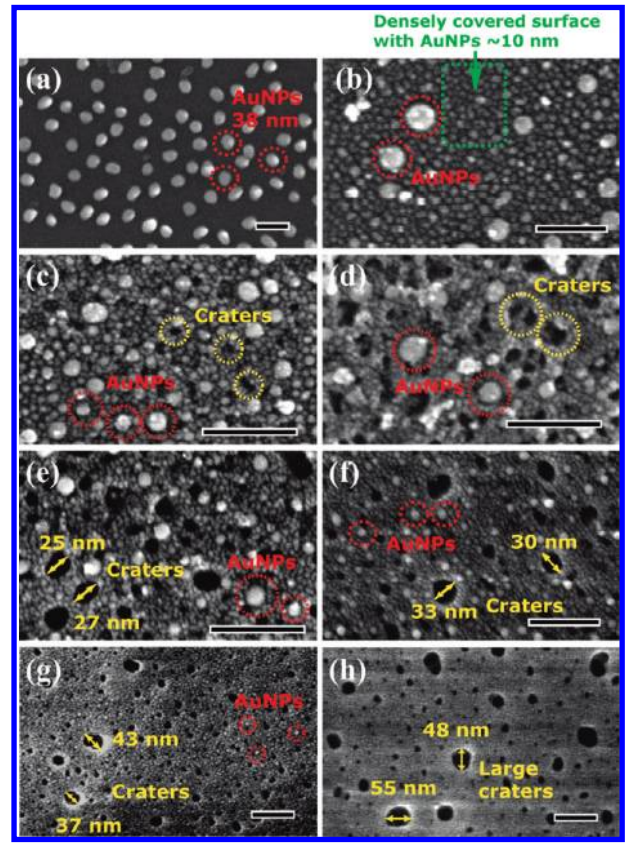

Figure 1. SEM observation of the evolution of craters on accumulated laser irradiation (532 nm, 6 ns, 470 mJ·cm^{-2}·pulse^{-1}) of a coverslip assembled with Au NPs (particle diameter: 38 ± 3 nm, surface coverage: 17.2%). Keys: (a) 0 shots, (b) 1 shot, (c) 5 shots, (d) 10 shots, (e) 30 shots, (f) 100 shots, (g) 200 shots, (h) 500 shots. The scale bars represent 100 nm. Au NPs (bright spheres) and craters (dark spots) in each shot number are marked in the images. The diameters of representative craters are also indicated for images e−h, suggesting the enlargement of crater diameters with increasing number of laser shots.

Results

Exposure of a glass substrate assembled with Au NPs to a 532 nm nanosecond pulsed-laser light allowed the observation of remarkable morphological alterations for both NPs and glass surfaces depending on the fluences and accumulated number of pulses. Figure 1 depicts the SEM images of the irradiated surfaces at a laser fluence of 470 mJ·cm^{-2}·pulse^{-1} with various laser shot numbers.

Before the laser irradiation, mostly well-separated Au NPs of 38 ± 3 nm diameter are deposited on the glass surface with a surface coverage of 17.2% (Figure 1a: bright spots marked with red circles). On irradiation of one laser shot (Figure 1b), Au NPs of less than 10 nm densely covered the surface (see, for instance, green-framed rectangle in Figure 1b) with some scattered intact (see bright spots marked with red circle) and aggregated (Supporting Information, Figure S1-1) Au particles. These particles hampered the explicit observation of a bare

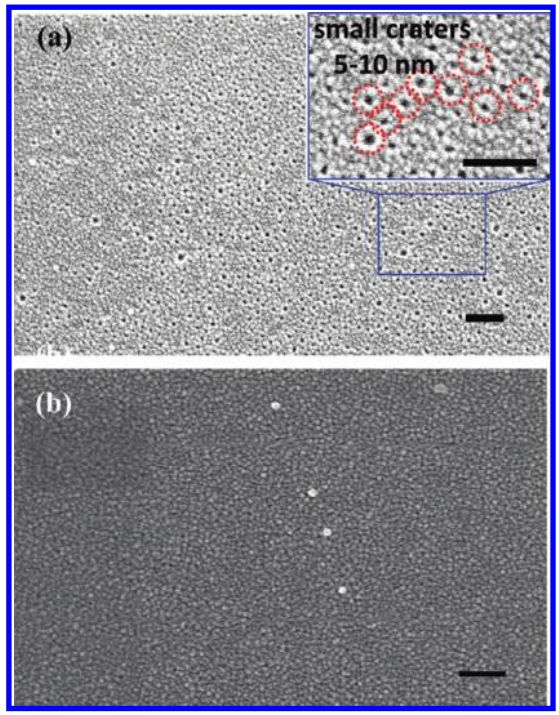

Figure 2. SEM observation indicating the crater formation on a glass substrate irradiated with one laser pulse (532 nm, 6 ns) after Au particles were removed by scraping with a cotton wiper moistened with methanol: (a) the SEM image irradiated at 460 mJ·cm^{-2}·pulse^{-1} exhibiting the occurrence of many small craters (inset: a magnified image of the specified area) and (b) the image irradiated at 90 mJ·cm^{-2}·pulse^{-1} exhibiting only a small number of craters present. A few bright spots in panel b show the Au particles remaining. The scale bars represent 100 nm.

surface; therefore, the SEM observation of the uncovered surface was made following the removal of Au particles after the one laser shot. As depicted in Figure 2a, small craters with sizes ranging from 5 to 10 nm diameter were formed in many different locations of irradiated area when the pulse energy is relatively high (460 and 370 mJ·cm^{-2}·pulse^{-1}). However, craters were hardly observed at a low pulse energy of 90 mJ·cm^{-2}·pulse^{-1} (Figure 2b).

The number density of craters is 4−5 times greater than that of the original Au particles, and the depths of the craters appears very shallow because they could easily disappear after prolonged exposure to an electron beam for the SEM measurements. After 5 laser shots, the craters were visible even without removing Au particles (Figure 1c, yellow circled spots, and Supporting Information, Figure S1-2 for the magnified image). The occurrence of the craters is more and more clearly detectable by increasing the laser shots (see the changes Figure 1d → e → f) along with the observation of a decreasing population of Au particles. It is noteworthy that some craters contain Au NPs inside (see magnified images for Supporting Information, Figure S1-3). Although the laser-induced splitting of the particles was a major observation,[27,28] the presence of large particles is evident, suggesting the growth or fusion of small particles simultaneously with the splitting. Further increase in the laser shots resulted in increased hole sizes (see the changes in particle diameters as marked in Figure 1e−h) in spite of the disappearance of Au NPs from the glass surface.

A quantitative aspect of the laser-induced crater formation at a laser fluence of 270 mJ·cm^{-2}·pulse^{-1} was summarized in Figure 3 by analyzing SEM images. Note here that the observation was made without removing Au particles after the irradiation.

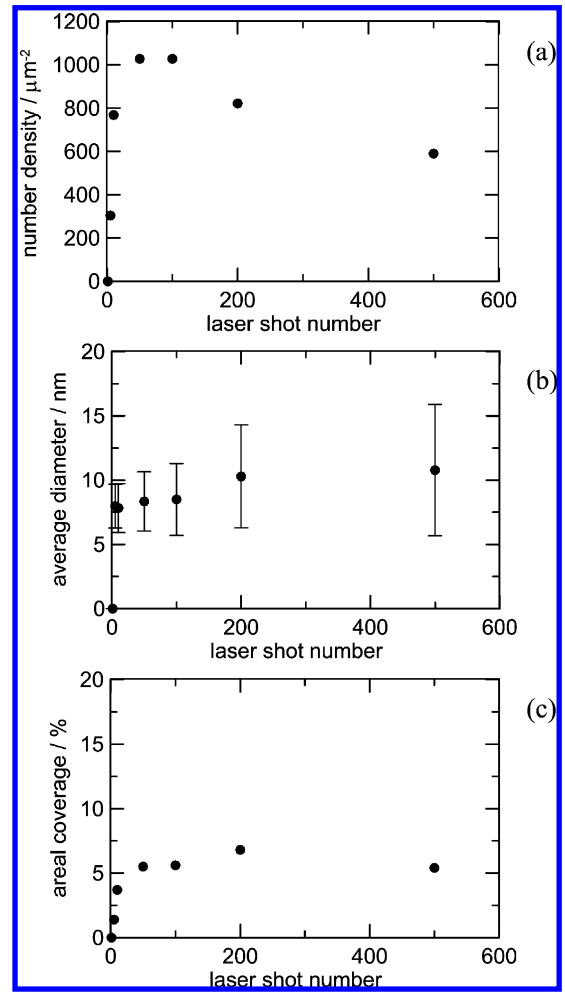

Figure 3. Accumulated laser shot number dependence of the number density (a), average diameter (b) and areal coverage (c) of craters formed on the laser-irradiated (532 nm, 6 ns, 270 mJ·cm^{-2}·pulse^{-1}) coverslip surface assembled with Au NPs (particle diameter: 42 ± 3 nm, surface coverage: 26.2%). The measurements were made without removing Au NPs.

At first, the number of craters increases with increasing number of laser shots but later it declines, as depicted in Figure 3a. This is because the size expansion takes place after accumulated irradiations, as shown in Figure 3b. On irradiating 500 laser shots, an average crater size of 10 ± 3 nm was obtained. One may notice the presence of much larger particles in the SEM pictures, as typically given in Figure 1h. However, because of a smaller fraction of such particles than that of much smaller particles, these particles contribute less to the calculated average sizes. Furthermore, a much lager size distribution of the crater diameter was noted at later stages. These observations suggest that the laser light stimulates craters residing nearby to combine to form new craters or encourages craters once produced to grow larger rather than acting to create new craters. The areal coverage of the craters steadily increased with increasing laser shot numbers until it leveled off (Figure 3c). The parameters given here, the number density, average diameter, and the areal coverage of the craters, were not affected by the laser fluence exceeding a certain threshold (see below). For instance, on irradiation of 500 shots at a fluence of 470 mJ·cm^{-2}·pulse^{-1} (for the sample in Figure 1), an average diameter of 13 ± 4 nm was obtained. The size enlargement of craters continued by further accumulation of laser shot numbers.

In order to gain insight into the events recorded by the SEM images, we measured the extinction (absorption and scattering)

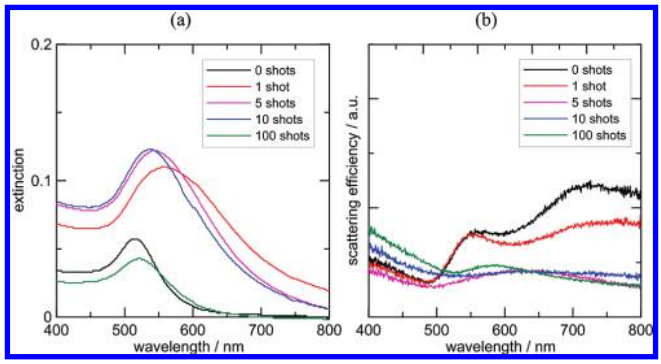

Figure 4. Extinction and scattering spectral modification due to 532 nm laser irradiation (470 mJ·cm^{-2}·pulse^{-1}) of a coverslip covered with Au NPs (particle diameter: ca. 40 nm, surface coverage: 19%).

and scattering spectra of the laser irradiated areas as a function of shot numbers. Figure 4a shows the evolution of extinction spectra, and Figure 4b shows that of the scattering spectra.

The extinction spectra are a measure of the size, number density, and extent of aggregation of Au particles, and the scattering spectra reflects the Au particle sizes and damages (holes) on the substrate surface. The former has significance in spectral intensity, but the latter is meaningful only in spectral shapes. Inspection of the both spectra reveals that the spectra certainly reflect the laser-induced modification of Au NPs. Before the laser irradiation, the extinction spectrum corresponding to a typical surface plasmon band of isolated Au NPs was recorded. The extinction spectral observation is roughly consistent with the SEM observation. On one shot of the laser irradiation, the extinction intensity increased remarkably with a shift to longer wavelengths, suggesting the formation of bigger or aggregated particles. Consistent with this observation, the visual inspection of the laser-irradiated areas of less than 10 pulses exhibited a bluish color. The SEM observation supports the presence of fused particles, but the number density of such particles was small. Rather, the SEM images revealed the dominance of closely packed small particles. For instance, the particle size of 10 ± 4 nm was obtained at 470 mJ·cm^{-2}·pulse^{-1} on one laser shot. These small particles may also contribute to the increased extinction intensity because of a densely packed structure. It has also been suggested that a gap-mode of the surface plasmon band can contribute to the enhanced extinction in the red region.[29]

On the other hand, the scattering spectrum of the intact sample exhibited a greater contribution of a band located at 700−800 nm ascribable to coupled or fused Au NPs. The presence of a nonnegligible amount of such coupled particles was evidenced by the SEM observation (Figure 1a, for instance, the center of three red circles). Thus the shape of the scattering spectrum is more sensitive to the aggregates than that of the extinction spectrum. The scattering spectra suggested the decreasing contribution of these large particles on one laser shot and subsequent accumulated irradiations due to the laser-induced pulverization.[27,28] With increasing laser shots, the extinction spectra gradually blue-shifted and then went down in intensity after the accumulation of a hundred shots due possibly to the disappearance of Au particles from the surface as observed by SEM images. Meanwhile, the scattering spectra after five shots of irradiation and later are dominated by a band with increasing intensity with decreasing wavelengths, which corresponds to a typical scattering spectrum (λ^{-4} dependence) of nonabsorbing materials.[30] This can be ascribed to the scattering by the craters formed on the glass surface. Note, however, that the extinction of Au NPs still exist even after 100 shots of irradiation.

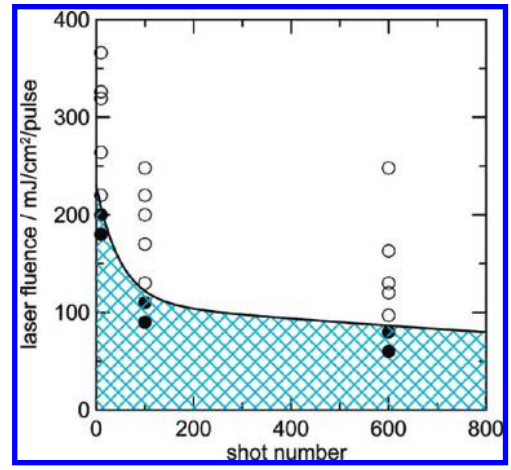

Figure 5. Threshold fluences of crater formation dependent on accumulated laser shot number for a laser-irradiated (532 nm) coverslip covered with Au NPs (particle diameter: ca. 40 nm, surface coverage: 17−23%).

The laser irradiation was carried out at various laser fluences along with varied number of laser shots. Notably, the crater formation took place even at a far less laser fluence than that observed in Figure 1. On the basis of the SEM observations, Figure 5 depicts plots of fluences at which the crater formation was observed (○) and not observed (●) as a function of the number of laser shots.

The solid curve in the figure represents a boundary or threshold of the crater formation. The result suggests that craters can form at a smaller number of laser shots as the fluence goes higher or an increasing number of laser shots are necessary to form craters with decreasing laser fluences. This implies that the crater formation is described by a stochastic event, and that more chances of craters are associated with higher fluences.

The laser-induced modification of both Au NPs and the substrate surface was assessed in further detail for better understanding of the phenomena by the close inspection of the SEM images. Figure 6 shows SEM pictures key to scrutinizing the mechanistic aspects of the crater formation.

Figure 6 a shows the radially arranged particles and craters that can be a signature of exploded fragments and openings hit by broken pieces. Unfortunately, we could not see the original particles before the laser excitation, and thus we have to speculate the event occurred after the laser excitation. It is pertinent to note that this image also shows moderate activity of Au particles associated with low laser fluences where only perfectly spherical Au particles of various sizes indicative of laser-induced melting were formed. Figure 6b shows the indication of a crater containing a few small craters inside. This image clearly shows the growth of craters is due to a sort of explosion of Au particles inside the crater. We have seen SEM pictures showing fragmented Au particles trapped in craters (Supporting Information, Figure S1−3). These trapped particles must be responsible for the crater size expansion. Additionally, we examined the effect of surface coverage by the observation of a substrate with a 1.2% coverage of Au NPs instead of the 17−23% normally employed. Both the fragmentation of the particles and damages to the substrate surface were observed (see Supporting Information, Figure S1−4) at fluences between 140 and 300 mJ·cm^{-2}·pulse^{-1}. However, the number density of the craters markedly reduced, suggesting that the original coverage of the surface by Au NPs is an important factor for the crater formation. Furthermore, no major difference was

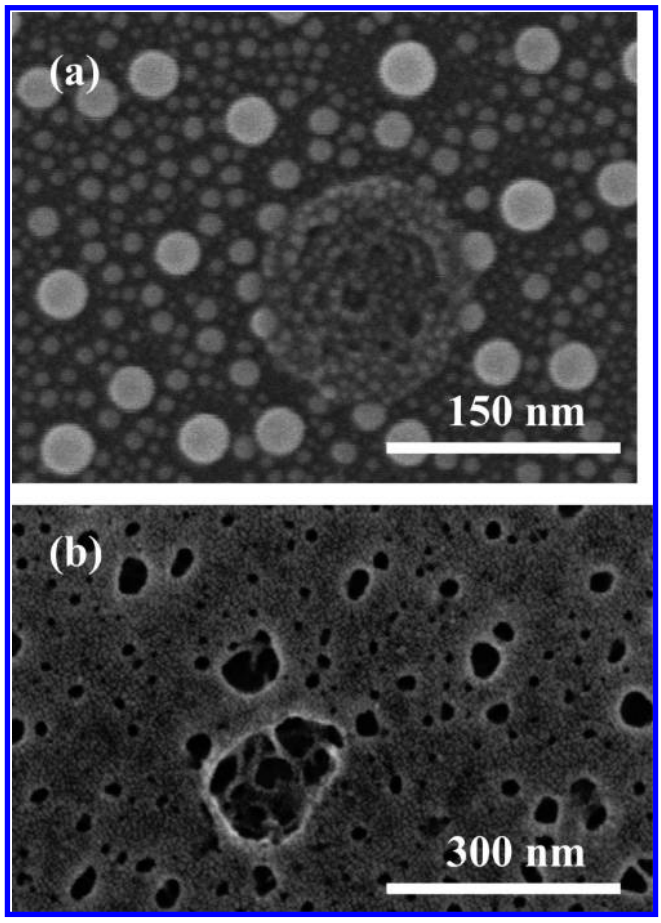

Figure 6. SEM images suggesting the growth mechanism of craters: (a) radially arranged particles and craters that can be a signature of exploded fragments and openings hit by broken pieces (90 $mJ \cdot cm^{-2} \cdot pulse^{-1}$, 600 shots), and (b) a crater containing a few craters suggesting the explosion of a particle inside the crater (350 $mJ \cdot cm^{-2} \cdot pulse^{-1}$, 100 shots).

observed for the surface modification when various sizes of Au particles ranging from 15 to 70 nm were employed with similar coverages.

After being subjected to accumulated laser irradiations, the photomodified areas were further processed by wet chemical etching in aqueous HF. The chemical etching technique allows the observation of structural or material changes due to exposure to the laser irradiation. For instance, heat-treated vitreous silica and femtosecond laser-treated various transparent inorganic materials including silica and borosilicate glasses were found to exhibit remarkable vulnerability to wet chemical etching by aqueous HF compared with untreated specimens.[31,32] For instance, it was reported that the etching rate of vitreous silica in 2.0% aqueous HF is 0.50 $\mu m \cdot h^{-1}$, while, on the other hand, a 100−200 enhanced etching rate was observed for the femtosencond laser exposed area.[33] The femtosecond laser technique was exploited to fabricate microchannels and micro-optical elements inside the transparent solids.[3,32] Thus the feasibility of chemical etching may open up the possibility of the structuring/processing of laser-exposed glass substrates modified with Au NPs. Figure 7 shows the observation of a pit due to the chemical etching of the laser exposed areas.

The laser modification was performed by exposure to various numbers of laser shots on a coverslip assembled with 40 nm Au NPs as shown in Figure 7a. The substrate was then submerged in 10% aqueous solution of HF at room temperature. The visual inspection of the HF-treated substrate reveals the

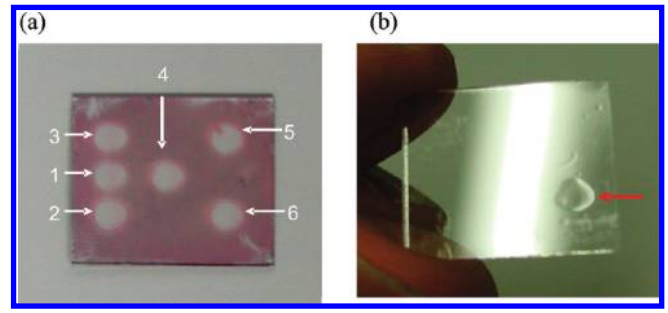

Figure 7. Au NP-assembled glass substrate after laser irradiation of various number of 532 nm laser shot at 380 $mJ \cdot cm^{-2} \cdot pulse^{-1}$ (a) and the same substrate after being submerged in 10% aqueous HF for 30 min (b). Keys: (1) 600 shots, (2) 1200 shots, (3) 1800 shots, (4) 3000 shots, (5) 6000 shots, (6) 18 000 shots. The red arrow in panel b indicates a 3 mm diameter crater formed by the etching of spot 6 in panel a.

formation of a ~3 mm diameter pit with a depth of at least several hundreds of micrometers. The surface of etched area was rather smooth. The position of the pit exactly matches the spot irradiated with 18000 shots (Figure 7b, the spot indicated by a red arrow corresponding to no. 6 in panel a). No visible pits were found with naked eyes for the rest of the laser exposed areas (nos. 1−5 in Figure 7a) after the chemical etching; however, the inspection of the substrate surface by a laser microscope showed the indication of etching. These pits were formed by etching with the aqueous HF possibly because of the higher etching rate of photomodified area within the substrate than that of intact glass.

Discussion

Excitation of the surface plasmon band of Au NPs has been suggested to give rise to two major outcomes. First, an effective coupling of the incident laser light to the plasmon oscillation allows a significant enhancement of the field, which can be absorbed by the substrate through a multiphoton process.[17] The enhancement is larger in the vicinity of associated or aggregated particles.[34] The multiphotonic process due to intense photon fields may result in the ablation and structural/material modifications of the substrate. The second possibility is the laser-induced heating of Au NPs.[27,35] On excitation of electrons due to the absorption of photons by the plasmon, instantaneous relaxation from plasmon to lattice takes place and the lattice phonon mode is excited. As a result, the temperature of Au NPs can be raised enormously. The heated Au NPs to temperatures well exceeding the boiling point (3243 K for bulk gold) may undergo explosive boiling causing pulverization.[27] This explosion may give a certain degree of damage to the glass substrate. Let us examine the mechanism of laser-induced crater formation on a glass substrate based upon the experimental observations.

Previously, Obara's group observed the formation of nanoholes on a silicon substrate by exciting Au NPs of 200 nm diameter spin-coated on the substrate by a single shot femtosecond pulsed-laser (λ = 820 nm, 100 fs, 140 $mJ \cdot cm^{-2}$) irradiation.[16−18] They concluded that near-field enhancement of Au NPs is responsible for this observation based on the fact that the nanohole profiles resembled the laser intensity distribution on the substrate surface in the fluence region lower than the ablation threshold fluence of the bulk silicon, and that the holes produced by a linearly polarized wave of laser radiation exhibited an elongated entrance shape in the direction of polarization. Similarly, Helzel and co-workers have demon-

strated that the irradiation of a single nanosecond laser pulse ($\lambda = 532$ nm, 10 ns, 50 mJ·cm^{-2}) on 250 and 50 nm Au spheres placed on a Si substrate (polished (100) surface with roughness of <2 nm) created nanoholes with the diameter of the spheres or slightly smaller.[20] They ascribed the formation of nanoholes to the optical excitation of plasmons leading to the field enhancement. The possibility of the heating of gold NPs was denied based on the fact that no such features were observed when the spheres were irradiated on the poly(methyl methacrylate) (PMMA) film spin-coated on a silicon substrate. Note here that the field enhancement by the excitation of plasmons is largely dependent on the dielectric function of a medium for a given size of Au NPs. On this point, a Si substrate is advantageous over SiO_2 or PMMA in terms of larger values of dielectric functions. For instance, the previous FDTD calculation predicted at least 8-fold enhanced electric field exerts for Si over SiO_2 on the substrate surface where a 200 nm Au sphere is placed.[17]

A question arises as to the fate of Au NPs in the above two cases because no descriptions was given to the particle after the nanohole fabrication. The photoexcitation of Au NPs results in both the absorption and scattering of photons; the former contributes to the generation of heat due to the processes of electron−electron scattering and electron−phonon scattering within the pulse duration while the latter contribute to the electric field enhancement in the near-field regime. According to the previous SEM images,[16−20] the Au spheres appeared to be disappeared from the field. However, we can imagine that the laser-induced splitting or melting of Au NPs is unavoidable in their system because the temperature rise due to photoabsorption can reach or even exceed the boiling point of Au. On this point, an approach by Tsuboi and co-workers is straightforward.[21] They irradiated a single shot nanosecond laser light (532 nm, 8 ns, 500−1000 mJ·cm^{-2}·pulse^{-1}) on 20 nm diameter Au NPs placed on a glass substrate and covered with a polymer film. They found that the formation of holes with a diameter of 30−70 nm accompanied by a complete disappearance of the particles. They discussed their result based upon the laser heating of Au NPs: the NPs were either vaporized or blown to pieces leaving holes as a trace of the NPs originally placed.

We observed the formation of nanosized craters on the nanosecond visible laser irradiation of Au NP-deposited glass substrates, but our observation is distinct from that of previous investigators. We observed the crater formation on glass substrates by a single-pulsed laser irradiation at relatively high laser fluences, but the crater sizes were very small and the number of craters exceeded that of original Au particles (see the difference between Figure 1a and Figure 2a). Here we look into the mechanism of photoinduced damages to the glass substrate. The possibility that the craters are formed by etching due to the enhanced electric field of light by the surface plasmon excitation is less likely because a one-on-one relationship between Au NP and crater could not be found. Laser-induced melting and splitting of Au NPs were found to be inevitable because of the heat resulting from light absorption on the excitation of the plasmon band. Here, we calculated the temperature rise of Au NPs with diameters of 15, 40, and 70 nm for one shot of a pulsed-laser and plotted it as a function of laser fluence in Figure 8.

The estimated temperature rise is enormous within the range of experimental laser fluences and the particle size dependence is rather small. According to this calculation, the laser energy of less than 30 mJ ·cm^{-2}·pulse^{-1} can raise the temperature of 40 nm Au particles to the boiling point and that of

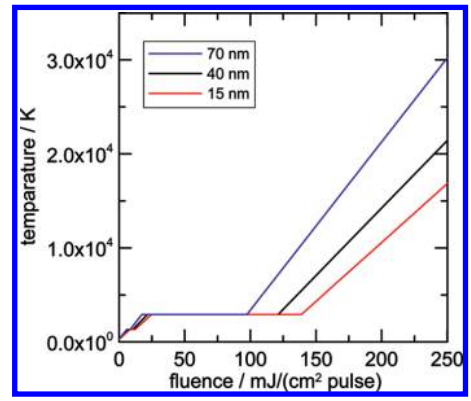

Figure 8. Calculated temperature rise for a single Au NP sphere with various diameters of 15, 40, 70 nm upon irradiation of one laser pulse (532 nm) as a function of laser fluence.

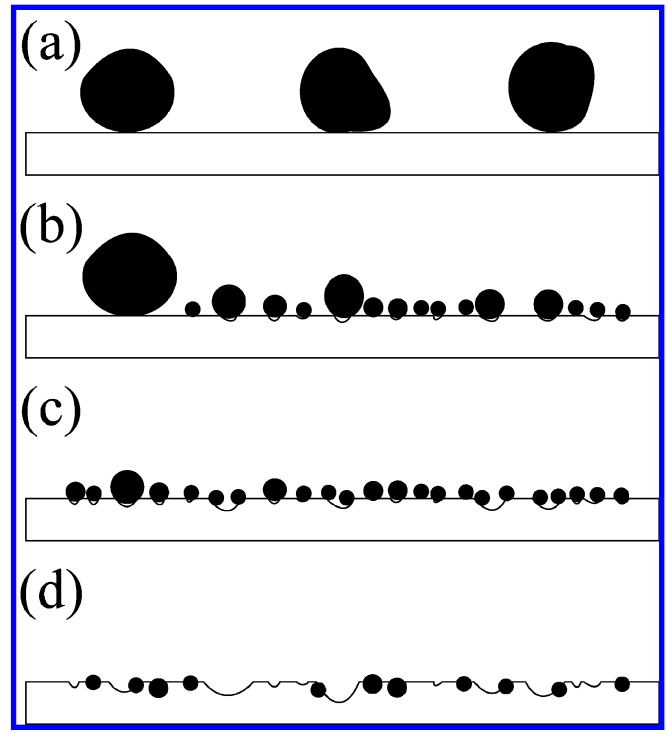

Figure 9. Schematic illustration of laser surface modification represented by the sequential cross sectional images of a Au NP-deposited glass substrate with increasing number of laser shots: (a) 0 shots, (b) 1 shot, (c) 5−100 shots, and (d) more than 100 shots.

120 mJ ·cm^{-2}·pulse^{-1}, over the boiling point. As depicted in Figure 5, we observed the laser shot number dependent damage threshold energies which always give rise to temperatures larger or equal to the boiling point. Therefore, we assume that the sudden heating of Au particles to boiling results in the surface modification of the glass substrate.

Let us now look into a plausible scenario for the laser-induced modification schematically illustrated in Figure 9.

Exposure to a pulsed-laser exceeding the ablation threshold brings about the splitting of Au NPs as observed in Figure 1. At the same time, it is likely that Au particles firmly fixed to the glass surface as a result of the excitation, according to the previous studies. For instance, Ito and co-workers found that a single Au NP placed on a glass substrate in aqueous solution adhere to the glass surface on laser splitting by a 532 nm nanosecond laser.[36] Niidome and co-workers observed the laser-induced deposition of Au NPs on the glass surface on excitation with 532 nm pulsed-laser irradiation of dodecanethiol-

protected Au NPs in cyclohexane.[37] Although not a glass substrate, Kawasaki and co-workers observed a similar strong adhesion of Ag and Au NPs to a mica substrate on repeated laser irradiation.[38] The mechanism of the attachment observed by these authors is still unclear, but we assume in our case the melting of a glass surface caused by heat transfer from Au NPs can play an important role. We observed a notable increase in the intensity of the extinction spectrum accompanied by a small red-shift at the initial stages of irradiation despite the fact that some portions of gold particles are likely to be blown away from the glass surface to the air. Nevertheless, the scattering spectra suggest a distinct trend that the fraction of large particles is decreasing on accumulating laser shots. Therefore, the increased extinction spectrum is ascribed to an increased dielectric medium surrounding Au NPs (see Supporting Information, Figure S3) because particles can be half-embedded in the glass substrate (Figure 9b). Thus we assume that the initial stage of the crater formation is due to the melting of the glass surface hit by laser-fragmented Au NPs with initial temperatures exceeding the boiling point. The explosion may account for a 4−5-fold increased number of small craters compared with the number of original Au NPs (see the difference between Figure 1a and Figure 2a). Meanwhile, we noted the presence of relatively large particles (Supporting Information, Figure S1-1) in addition to the small particles (Figure 1b). These large particles must be formed by the fusion of small particles resulting from the splitting and may contribute significantly to the crater formation because of high temperature. The next step is the enlargement of craters due to the accumulated laser irradiation. This is due to the explosive splitting of Au NPs residing in craters (Figure 9c → d). We saw frequently the SEM pictures showing the craters containing Au NPs (Supporting Information, Figure S1-3). Besides this, we captured the SEM image of small craters inside a crater as typically depicted in Figure 6b. By further increasing the laser shot numbers, we see less number of Au NPs exposed to the glass surfaces. At this stage, the number of craters showed no further increase; however, the enlargement of the crater size still proceeds. For instance, craters as large as 100 nm diameter were formed after 18000 shots.

We observed enhanced wet chemical etching of the laser-exposed areas assembled with Au NPs (Figure 7). The previous studies revealed that the heat-, laser- and radiation-induced densification of vitreous silica is responsible for acquiring greater etching susceptibility to aqueous HF.[31,33,39,40] Such densification has been assessed by the measurement of Raman spectra.[33,41−44] Hence, we measured the Raman spectra of the laser-exposed area in order to gain insight into the etching mechanism. For this purpose we used vitreous silica instead of borosilicate glass as a substrate for the Au NP assembly because previous Raman spectroscopic results are available only for quartz. Our preliminary result was given in the Supporting Information, Figure S4. We observed increased intensities of the band located at 490 cm^{-1} (D_1) while no increase was observed for the band located at 605 cm^{-1} (D_2). Here, because of unexpectedly strong emission from laser-exposed areas, we were forced to use the excitation wavelength of 1064 nm, which is disadvantageous in the detection sensitivity of Raman signals. It has been revealed that the D_1 band is assignable to the ring-breathing mode of four-membered siloxane rings in silica, and D_2 band is assignable to the three-membered O−Si−O rings.[41−44] These small ring structures were considered unstable and reactive toward HF compared with six-membered ring structures of amorphous silica.[31] It is particularly noteworthy that Awazu observed the intensification of the D_1 band of vitreous silica exposed to a 193 nm ArF excimer laser.[44] This finding is similar to our present observation (Supporting Information, Figure S4). He concluded that the flash heating of silica by the UV laser irradiation is largely responsible for the observed increase in the intensity of D_1 band. Thus, the photomodification leading to the subsequent chemical etching in our present system is safely ascribed to the surface heating, which brings about an increased fictive temperature. Another example supporting this conclusion is a CW 10.6 μm CO_2 laser-treated silica glass that allowed a facile wet etching by HF.[45] We note here that the degree of modification by exposure to the nanosecond UV laser is less remarkable than that observed for quartz exposed to femotosecond NIR lasers, which bring about the intensification of the D_2 band and thus lead to a higher fictive temperature of the irradiated area.

The present assumption of laser heating-induced photomodification of the substrate surface giving rise to the enhanced chemical etching is consistent with our picture of Au NP-induced laser surface damage caused by excessively heated NPs mentioned above. One may wonder why the volume removed by HF etching is much larger than the depth of photomodified area, which is expected to be less than a micrometer. However, this type of etching behavior is frequently observed in the area of femtosecond laser processing.[33] The etching by HF occurs initially within the laser-exposed volumes but later penetrates to the neighboring areas surrounding them, rendering the diameters of channels much larger than those exposed to the lasers. Most important observation made by us is that the areas exposed relatively low intensity lasers are entirely removed by HF etching, which makes the method promising for a new type of energy saving laser processing.

Summary

The present study is regarded as the extension of the laser ablation of Au NPs in solution[27,28] to the solid surface where the substrate serves as a heat sink. In addition to the laser-induced splitting and fusion of Au NPs on a glass substrate, the surface modification represented by a large number of craters with less than 10 nm diameter were observed at scattered places on one shot of a 532 nm nanosecond pulsed-laser beam. The repeated irradiation granted the size expansion of the craters. The present observation of craters is distinct from the previous observation of nanoholes on a silicon substrate, where a single laser shot allowed the fabrication of the pit just underneath a given Au NP due to the plasmonic enhancement of the electromagnetic field.[16−20] The mechanism of the present crater formation was ascribed primarily to the laser-heating of the particles causing a melting of the glass surface resulting from heat transfer from gold particles to the host material followed by a drilling due to the explosion of the laser-heated particles. Thus the excess energy originating from the excitation of Au NPs was delivered to the medium for the surface modification, which is a process unexpected from the previous solution studies. Interestingly, the laser-modified area acquired the etching susceptibility to aqueous HF and the selective etching of the area was attained. The result strongly suggests the feasibility of Au NP-based laser structuring on glass substrates if a more sophisticated control was achieved to the fabrication of NP assemblies and to the laser irradiation conditions including the application of photomasks.

Acknowledgment. Financial support by the Nippon Sheet Glass Foundation for Materials Science and Engineering

(Research Grant 2008) and KAKENHI on Priority Areas "Strong Photon−Molecule Coupling Fields (No. 470) # 21020025" and "Molecular Science for Supra-Functional Systems (No. 477)" from the MEXT of Japanese government is gratefully acknowledged. The MOE-ATU Project (National Chiao Tung University) administrated by the Ministry of Education, Taiwan, and National Science Council of Taiwan (0970027441) are also acknowledged for financial support.

Supporting Information Available: Magnified images of Figure 1, SEM image for 1.2% coverage sample, calculated extinction spectra of a 40 nm Au sphere dependent on the refractive index of medium, Raman spectra of 532 nm laser-irradiated quartz substrate assembled with 40 nm Au NPs, and a note describing the evaluation of laser-induced temperature rise of Au NPs. This material is available free of charge via the Internet at http://pubs.acs.org.

References and Notes

(1) Bauerle, D. *Laser Processing and Chemistry*, 3rd ed.; Springer-Verlag: Berlin, 2000.
(2) Gattass, R. R.; Mazur, E. *Nat. Photonics* **2008**, *2*, 219–225.
(3) Juodkazis, S.; Mizeikis, V.; Matsuo, S.; Ueno, K.; Misawa, H. *Bull. Chem. Soc. Jpn.* **2008**, *81*, 411–448.
(4) Kreibig, U.; Vollmer, M. *Optical Properties of Metal Clusters*; Springer: Berlin, 1995.
(5) Ricard, D.; Roussignol, P.; Flytzanis, F. *Opt. Lett.* **1985**, *10*, 511–513.
(6) Chakraborty, P. *J. Mater. Sci.* **1998**, *33*, 2235–2249.
(7) Maier, S. A. *Curr. Nanosci.* **2005**, *1*, 17–22.
(8) Haes, A. J.; Stuart, D. A.; Nie, S.; Van Duyne, R. P. *J. Fluoresc.* **2004**, *14*, 355–367, and references therein.
(9) Olk, P.; Renger, J.; Hartling, T.; Wenzel, M. T.; Eng, L. M. *Anal. Chem.* **2002**, *74*, 504–509.
(10) Kityk, I. V.; Ebothe, J.; Fuks-Janczarek, I.; Umar, A. A.; Kobayashi, K.; Oyama, M.; Sahraoui, B. *Nanotechnology* **2005**, *16*, 1687–1692.
(11) Debrus, S.; Lafait, J.; May, M.; Pincon, N.; Prot, D.; Sella, C.; Venturini, J. *J. Appl. Phys.* **2000**, *88*, 4469–4475.
(12) Pieczonka, N. P. W.; Aroca, R. F. *Chem. Soc. Rev.* **2008**, *37*, 946–954.
(13) Etchegoin, P. G.; LeRu, E. C. *Phys. Chem. Chem. Phys.* **2008**, *10*, 6079–6089.
(14) Geddes, C. D.; Lakowicz, J. R. *J. Fluoresc.* **2002**, *12*, 121–129.
(15) Lakowicz, J. R. *Plasmonics* **2006**, *1*, 5–33.
(16) Nedyalkov, N. N.; Takada, H.; Obara, M. *Appl. Phys. A: Mater. Sci. Process.* **2006**, *85*, 163–168.
(17) Nedyalkov, N. N.; Sakai, T.; Mianishi, T.; Obara, M. *J. Phys. D: Appl. Phys.* **2006**, *39*, 5037–5042.
(18) Atanasov, P. A.; Takada, H.; Nedyalkov, N. N.; Obara, M. *Appl. Surf. Sci.* **2007**, *253*, 8304–8308.
(19) Leiderer, P.; Bartels, C.; Konig-Birk, J.; Mosbacher, M.; Boneberg, J. *Appl. Phys. Lett.* **2004**, *85*, 5370–5372.
(20) Heltzel, A.; Theppakuttai, S.; Chen, S. C.; Howell, J. R. *Nanotechnology* **2008**, *19*, 025305.
(21) Yamada, K.; Itoh, T.; Tsuboi, Y. *Appl. Phys. Express* **2008**, *1*, 087001.
(22) Papernov, S.; Schmid, A. W. *J. Appl. Phys.* **2002**, *92*, 5720–5728.
(23) Kim, T. H.; Lee, K. H.; Jung, Y. H.; Kim, Y. S.; Chin, H. J.; Ryu, B. K.; Kang, H. O.; Lee, S. H. *J. Ceram. Soc. Jpn.* **2008**, *116*, 309–312.
(24) Wang, J.; Niino, H.; Yabe, A. *Appl. Phys. A: Mater. Sci. Process.* **1999**, *68*, 111–113.
(25) Frens, G. *Nature Phys. Sci.* **1973**, *241*, 20–22.
(26) Keating, C. D.; Musick, M. D.; Keefe, M. H.; Natan, M. J. *J. Chem. Educ.* **1999**, *76*, 949–955.
(27) Takami, A.; Kurita, H.; Koda, S. *J. Phys. Chem. B* **1999**, *103*, 1226–1232.
(28) Mafune, F.; Kohno, J.; Takeda, Y.; Kondow, T. *J. Phys. Chem. B* **2001**, *105*, 5114–5120.
(29) Ueno, K.; Juodokazis, S.; Mizeikis, V.; Sasaki, K.; Misawa, H. *Adv. Mater.* **2008**, *20*, 26–30.
(30) Yguerabide, J.; Yguerabide, E. E. *Anal. Biochem.* **1998**, *262*, 137–156.
(31) Agarwal, A.; Tomozawa, M. *J. Non-Cryst. Solids* **1997**, *209*, 166–174.
(32) Marcinkevius, A.; Juodkazis, S.; Watanabe, M.; Miwa, M.; Matsuo, S.; Misawa, H.; Nishii, J. *Opt. Lett.* **2001**, *26*, 277–279.
(33) Kiyama, S.; Matsuo, S.; Hashimoto, S.; Morihira, Y. *J. Phys. Chem. C* **2009**, *113*, 11560–11566.
(34) Kneipp, K.; Kneipp, H.; Bohr, H. G. *Top. Appl. Phys.* **2006**, *103*, 261–278.
(35) Pyatenko, A.; Yamaguchi, M.; Suzuki, M. *J. Phys. Chem. C* **2009**, *113*, 9078–9085.
(36) Ito, S.; Mizuno, T.; Yoshikawa, H.; Masuhara, H. *Jpn. J. Appl. Phys.* **2007**, *46*, L241–L243.
(37) Niidome, Y.; Hori, A.; Takahashi, H.; Goto, Y.; Yamada, S. *Nano Lett.* **2001**, *1*, 365–367.
(38) Kawasaki, M.; Hori, M. *J. Phys. Chem. B* **2003**, *107*, 6760–6765.
(39) Hnatovsky, C.; Taylor, R. S.; Simova, E.; Rajeev, P. P.; Rayner, D. M.; Bhardwaj, V. R.; Corkum, P. B. *Appl. Phys. A: Mater. Sci. Process.* **2006**, *84*, 47–61.
(40) Bellouard, Y.; Barthel, E.; Sais, A. A.; Dugan, M.; Bado, P. *Opt. Express* **2008**, *16*, 19520–19534.
(41) Chen, J. W.; Huser, T.; Risbud, S.; Krol, D. M. *Opt. Lett.* **2001**, *26*, 1726–1728.
(42) Kucheyev, S. O.; Demos, S. G. *Appl. Phys. Lett.* **2003**, *82*, 3230–3232.
(43) Awazu, K.; Kawazoe, H. *J. Appl. Phys.* **2003**, *94*, 6243–6262.
(44) Awazu, K. *J. Non-Cryst. Solids,* **2004**, *337*, 241–253.
(45) Zhao, J.; Sullican, J.; Bennett, T. D. *Appl. Surf. Sci.* **2004**, *225*, 250–255.

JP905291H